Numerical Simulation of Electrohydraulic Forming of Aluminium Alloy Tubes

Q. L. Zheng[1], H. P. Yu[1*]

[1]School of Materials Science & Engineering, Harbin Institute of Technology, Harbin 150001 China
*Corresponding author: E-mail: haipingy@hit.edu.cn

Abstract

Electrohydraulic forming has the advantages in improving formability and deformation precision of the workpiece, so it is concerned and applied in the plastic deformation for high precision parts, which are made of sheet or tube and difficult to form by traditional methods. However, electrohydraulic forming is based on a coupled effect of gaseous, liquid, and solid media and materials, and its states cannot be identified by experiments alone. Therefore, this paper takes the local bulging deformation behaviour of 5052 aluminium alloy tubes as the research object, used FEM software ANSYS/LS-DYNA to establish the numerical simulation model, and studied the plastic deformation behaviour of tubes under the action of shockwave load during electrohydraulic forming.

Keywords

Electrohydraulic forming, Numerical simulation, Aluminium alloy tubes

1 Introduction

In recent years, with the rapid development of aerospace, large machinery, transportation and other fields, the industry has put forward higher and higher requirements on the overall weight reduction. The materials such as lightweight alloys (magnesium alloys, aluminium alloys) have been widely applied in industry(Kang,2008). But these materials suffer from poor formability at room temperature. Electrohydraulic forming (EHF) is a typical high speed forming technology which can improve the formability of those lightweight materials. When controlled quantities of electrical energy are stored and then released instantaneously into a bridge wire, a transformation occurs. The electrical energy vaporizes

the bridge wire submerged in the liquid water, and a small explosion takes place. Shock waves emanating from the explosion move outward in all directions and can be controlled to produce deformation in a metal workpiece (Bruno, 1968). A significant advantage of EHF compared to traditional sheet metal forming technology is that it does not require two matching dies: a punch is usually replaced by liquid, transmitting pressure from the discharge channel to the surface of the blank. At present, electrohydraulic forming technology has been applied in many fields. It can be used for forming complex shape parts or multi-mode parts (Gong,1984; Zhang et al., 1997), and also can be used in the field of calibration (Golovashchenko et al., 2014). Electro hydraulic forming of a range of different sheet steels was studied experimentally by (Melander et al., 2013), and a finite element model was formulated in ABAQUS explicit, and the model shows satisfactory results in relation to the experimental trials regarding both shape and strains of the pressed sheets. Electrohydraulic die-forming (EHDF) and free-forming (EHFF) of DP590 dual phase steel were simulated in ABAQUS/Explicit to investigate the effect of released energy on the sheet deformation profile history, strain distribution, loading path and damage accumulation type, and the predicted final strain values and damage accumulation type showed good agreement with the experimental observations (Hassannejadasl et al., 2014).

Therefore, electrohydraulic forming is suitable for the deformation of those hard deformable materials at room temperature, and numerical simulation technology was also used to assist the experimental results. (Hajializadeh and Mashhadi, 2015; Mamutov et al., 2015) had conducted the investigation and numerical simulation of impulsive hydroforming of aluminium tubes, but they didn't compare the numerical simulation results with the experimental results. So this paper takes the local EHF bulging of 5052 aluminium alloy tubes as the research object, uses the finite element analysis software ANSYS/LS-DYNA to establish a reasonable model to quantitatively analyze the process of production and propagation of the shockwave and the deformation process of tubes, and uses the numerical simulation results to quantitatively analyze the variation of stress, displacement and velocity versus time of the EHF process.

2 Experimental procedure

2.1 Specimen preparation and EHF apparatus

Annealed 5052 aluminium alloy tubes are used for EHF bulging experiments. The tube is 104mm long, possesses an outer diameter of 50mm and a wall thickness of 1.2mm. The yield strength, tensile strength and elongation rate are 95.68MPa, 184.81MPa and 28.86%, respectively.

Bulging experiments of EHF for aluminium alloy tubes were carried out using a pulsed discharge device with the capacitance of 100μF and rated discharge voltage of 20kV. In order to enable the extraction of the deformed tube parts, the die has two halves,

the shape and dimensions are shown in Fig. 1(a). The diameter of both cylindrical ends of the die is 50mm so that to match the outer diameter of tube blanks. In Fig. 1(a), the A, B and C are corresponding to the cylindrical region, the straight wall and the fillet area in turn. The schematic diagram of EHF setup is shown in Fig. 1(b) and the experimental setup is shown in Fig. 1(c). The positive and negative electrodes, spacing 18mm, are mounted on the upper cover plate of EHF setup, and insulated from die halves by a nylon sleeve. In order to improve the efficiency of an EHF process, a short metal wire is connected between both electrodes before discharge. And an electric explosion of metal wire takes place when a high voltage pulsed current flows through it during the discharge. Consequently, the metal wire is also called as the electric exploding wire.

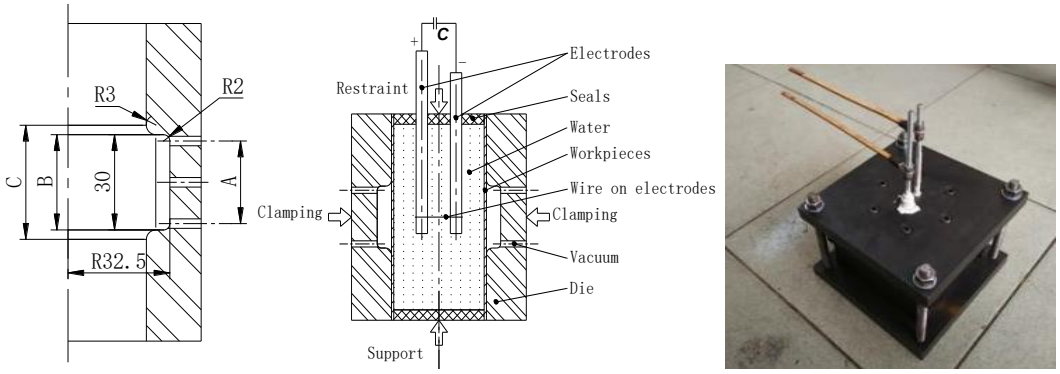

(a) *(b)* *(c)*

***Figure 1**: (a) Dimensions of die cavity(unit: mm) (b) Schematic diagram of EHF (c) Experimental setup*

2.2 The experimental results

The pure aluminium wire with a diameter of 0.6mm is chosen as the electrical explosion wire. The EHF tubes under varied discharge voltage (3kV~9kV) and their profiles are presented in Fig. 2. It can be seen from the figure that the radial bulging is the smallest under the discharge voltage of 3kV, and is far from the attaching-die state. When the discharge voltage is up to 4kV, the wall in the middle of deformed tube begins to just contact with the inner surface of die cavity. With the increase of the discharge voltage, the contacting area between the bulged part of tubes and the die extends along the generatrix of cylindrical region of die, and then begins to fill the fillet area of die cavity. When discharge voltage increased to 9kV, the deformed tube presents a good attaching die result and no cracks happen in deformation zone.

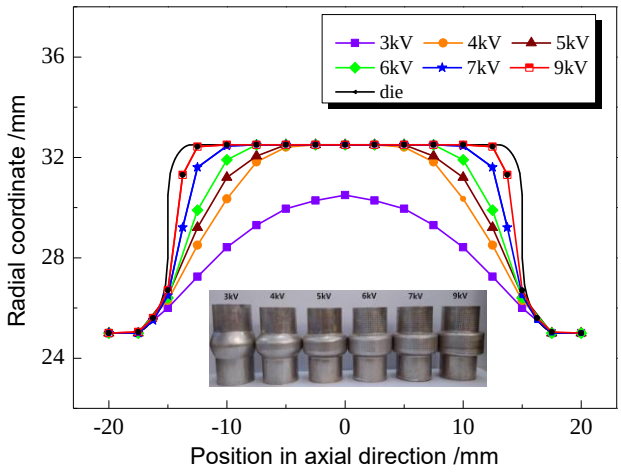

***Figure 2**: Deformed tubes and profile curves under varied discharge voltages*

3 Numerical simulation of EHF

3.1 Model of numerical simulation

In order to better understand the deformation mechanism and forming process in EHF, numerical modelling was performed by FEM software ANSYS/LS-DYNA for EHF 5052 aluminium alloy tubes. We adopt the following models implemented by (Golvashchenkoet al., 2013), and the material models for each model are shown in parentheses: (1) Electrical model of the discharge channel; (2) Model of plasma channel (*MAT_NULL); (3) Model of the liquid as a pressure transmitting medium (*MAT_NULL); (4) A deformable tube in contact with a rigid die (a Prezyna: *MAT_PLASTIC_KINEMATIC_TITLE); (5) Model of ambient air (*MAT_NULL); and (6) Rigid die (*MAT_RIGID_TITLE). Here obtains the numerical coupling of models for the gas, solid and liquid phase through the keyword *CONSTRAINED_LAGRANGE_IN_SOLID_TITLE.

The electric power being pumped through the discharge channel can be defined by the following equation (Golvashchenko et al., 2014):

$$N = i(t) \cdot U(t) \tag{1}$$

where *i(t)* and *U(t)* – are the current and voltage as measured by an oscilloscope across the electrodes, respectively. The electric current is measured by a gauged Rogowski coil while voltage is measured across the ends of the electrodes outside the EHF chamber.

The starting time of the energy input into the simulation is not specifically indicated in the paper of (Mamutov et al., 2015), and this information is important. In this paper, the curve of electric power versus time is shown in Fig. 3,it must be emphasized that the starting time of the energy input into the simulation is 7.4μs not 0μs. Before the 7.4μs, the energy input into the metal wire is used to achieve the phase transitions and do not work on

the tube; After 7.4μs, the plasma channel is broken down, then the shockwave begins to work on the tube.

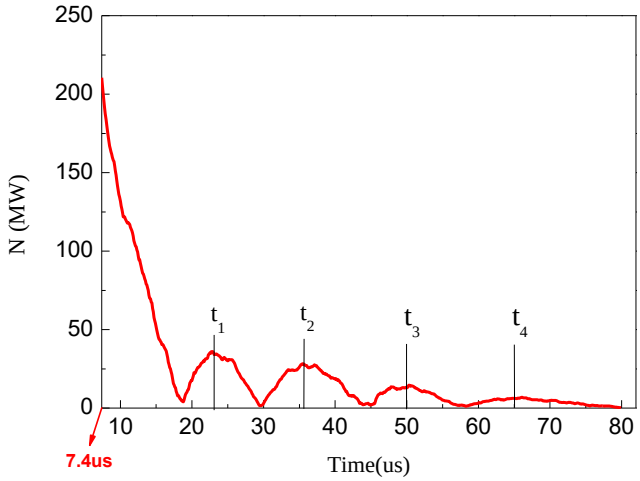

***Figure 3**: The curve of the power-time input into the channel (6kV)*

The plasma channel is modelled in LS DYNA as an adiabatically expanding volume of gas. The electric energy is assumed to be introduced uniformly through the channel volume. The liquid is modelled within LS DYNA as an ideal compressible liquid with the specific cavitation threshold. Modelling of the tube formed into the die cavity is conducted using elastic-plastic solid elements incorporating bending stiffness and being in contact with a rigid die. The 3D model and dimensions of each part shown in Fig.4 are in accordance with the experimental dimensions, and the plasma channel is a cuboid with 2mm×2mm×14mm.

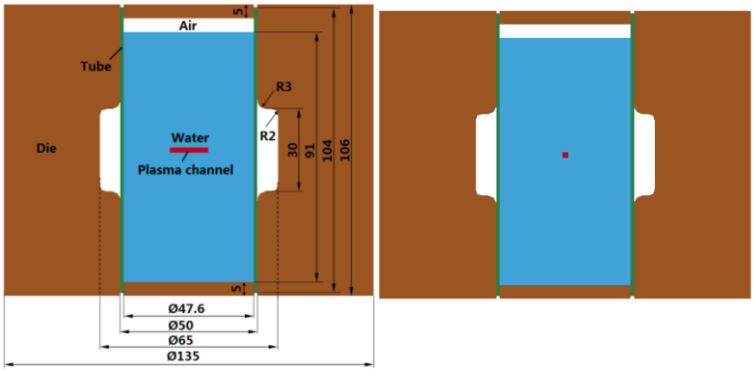

***Figure 4**: The cross-section model and dimensions of each part (unit: mm)*

3.2 Results and discussion of numerical simulation

The simulation results of EHF 5052 aluminium alloy tube with discharge voltage of 7kV are shown in Fig. 5 (contours of dominant fluid material). In order to intuitively observe the flow of the fluid and the deformation trend of tube, the die is hidden here. It can be

seen from the figure that the discharge channel, which turns into an overheated plasma/vapour mixture, expands substantially during the process and generates the shockwave. The shape of the shockwave is close to the ellipsoid firstly, the major axis is along the axial direction of the metal wire, the minor axis is along the radial direction of the geometric centre of the metal wire, and as the shockwave rapidly spreads, the shockwave becomes closer to the sphere, which delivers pulsed pressure to the surface of the tube and accelerates the tube toward to the die cavity. The fluid can flow to each other during the process of deformation due to the coupling arrangement of gas-liquid-solid phase. Therefore, results from the numerical simulation illustratesa rather complex mechanism within the EHF process.

The original height of tube amounts to 104mm and the height of the experimentally deformed tube is 97.5mm, yielding a difference of 6.5mm. The height of the deformed tube according to numerical simulation is 97.8 mm, with a difference of 6.2mm, yielding a relative error of 4.62%. The deviations between the experimental results and numerical simulation are relatively small. Therefore, this work utilizing the results of numerical simulation to analyze the EHF deformation process proves feasible.

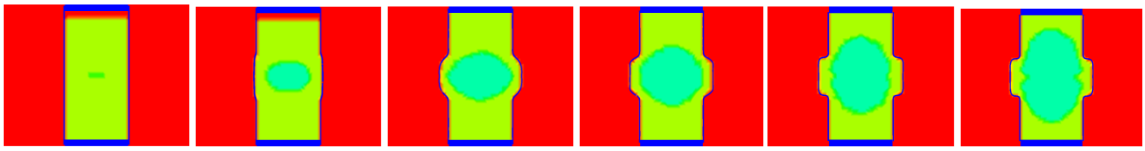

t=0μst=30μs t=70μst=100μst=150μs t=200μs

***Figure 5**: The EHF process of 5052 aluminium alloy tube*

In order to observe the changes of the stress, displacement and velocity of the tube over time, the elements A, B, C, D and E on the outer surface of the tube are taken as the research objects. Comparing the curves to further understand the deformation behaviour of tube under the action of shockwave load and hydrodynamic pressure. The results are shown in Fig.6- 8.

In (Hajializadeh and Mashhadi, 2015; Mamutov et al., 2015), they all concern the distribution of the pressure in the cylindrical chamber at different times, but they don't pay attention to stress of the tube. Fig.6 are the curves of effective stress-time of the investigated elements, from the figure we can see that the shockwave has a larger impact force on the tube at the beginning of EHF, and the equivalent stress of the elements increases rapidly, of which the equivalent stress of the element C located at the centre of the tube is the largest (about 7μs-10μs). After 10μs, the tube begins to deform, and the equivalent stress of element B,C,D continues to increase, but the slope decreases slightly; At this time, the elements A and E located at the fillet of the die contact the die and are subjected to the reverse extrusion, so the equivalent stress decreases; About 75μs, element C located at the centre of the tube impacts the die, and the equivalent stress momentarily increases to the peak. With the attenuation of energy, the integral equivalent stress of the tube decreases gradually. After the EHF process, the equivalent stress of the tube don't

reduce to zero immediately due to the pressure maintaining effect of the liquid medium water.

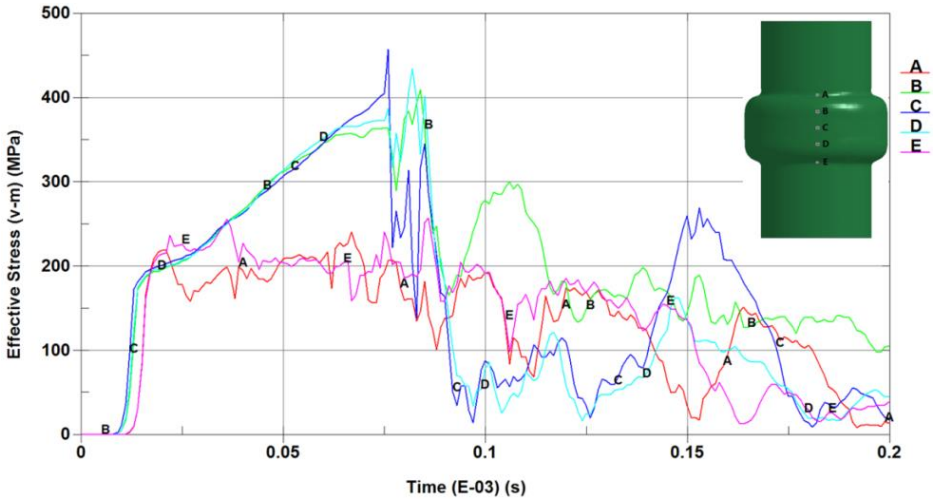

***Figure 6**: The curves of effective stress -time*

Fig.7 are the curves of resultant displacement-time of the investigated elements, it can be seen from the figure that the tube begins to deform at about 10μs. Under the action of the shockwave load, the displacement of the element B,C,D located at the centre of the tube are larger than the displacement of the element A,E located at the fillet of the die, and the displacement of the element C is the largest. About 75μs, element C located at the centre of the tube impacts the die, and the displacement increases to the peak. Then the impact results in a slightly rebounded phenomenon, so we can see that the displacement of the element C decreases slightly after the 75μs, and finally tends to a steady state. With the continuation of the deformation, the element B,D attach the die wall also, and the displacement of element A,E increases gradually and tends to a steady state. The changes in displacement are also mentioned in (Hajializadeh and Mashhadi, 2015), but they only shows the result of the centre node of the blank (dome height).

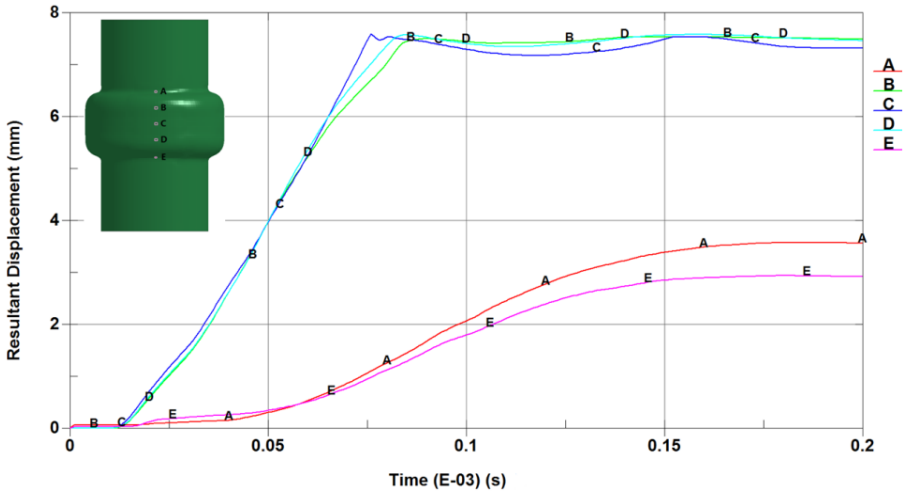

***Figure 7**: The curves of resultant displacement-time*

The resultant velocity of various elements are not mentioned in (Hajializadeh and Mashhadi, 2015; Mamutov et al., 2015), but it is necessary to investigate this result during EHF process. Fig.8 are the curves of resultant velocity -time of the investigated elements, it can be seen from the figure that the tube begins to deform at about 10μs and the velocity of the element B,C,D increases momentarily. About 75μs, element C located at the centre of the tube impacts the die, and the velocity decreases momentarily. Then with the attenuation of energy, the integral velocity of the tube decreases gradually. After the EHF process, the velocity of the tube reduces to zero. The velocity of each element fluctuates before the tube contacts the die, which was mainly caused by the energy attenuation and the decrease of the amplitude of the shock wave. So the slope of the velocity gradually slows down also, and the time of the peak of the velocity is almost in accordance with the t_1, t_2, t_3, t_4 shown in Fig.3.

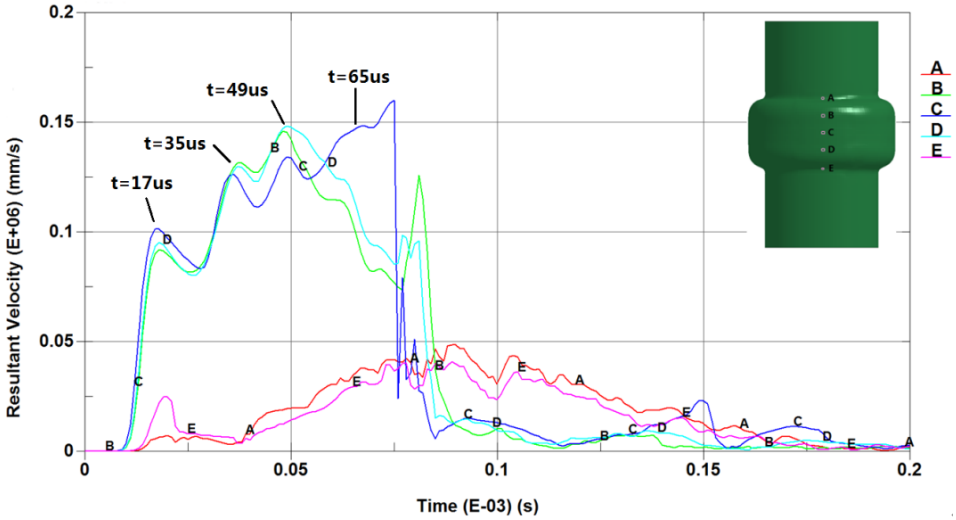

***Figure 8**: The curves of resultant velocity-time*

The starting time of the energy input into the simulation of this paper is 7.4 μs not 0 μs. And the results of the numerical simulation are in accordance with the experimental results, as shown in Section 3.2. In order to further prove the accuracy of the initial energy input into the simulation, under the conditions of the discharge voltage of 5kV, there performs numerical simulation of EHF tube with the starting time of the energy input is 0μs. The contours of effective plastic strain of tubes are shown in Fig.9. For the picture on the right, because the energy used for phase transitions is also used to work on the tube, so the effective plastic strain is larger than that of the left tube, and the deformation is far greater than the experimental results with the discharge voltage of 5kV.

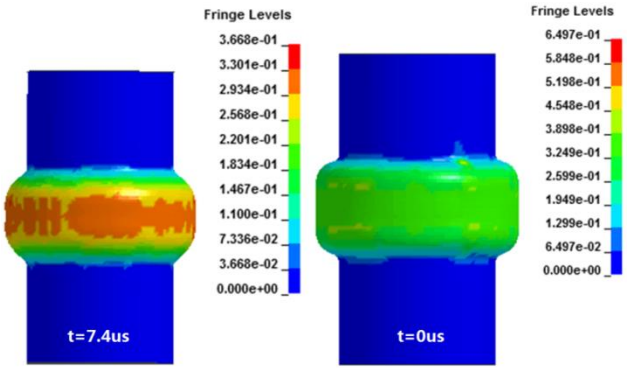

***Figure 9**: The contours of effective plastic strain of EHF tubes*

We performs numerical simulations of electrohydraulically formed tubes under varied discharge voltage (3kV - 7kV), and there compares the results of experiments and numerical simulation, the results are shown in Fig.10. From the attaching-die capability we can see that the results of numerical simulation are in quite accordance with the experimental results, the error is in the range of 0-5%, and this result further demonstrates the feasibility of using numerical simulation to analyze the EHF process presented in the Section 3.2.

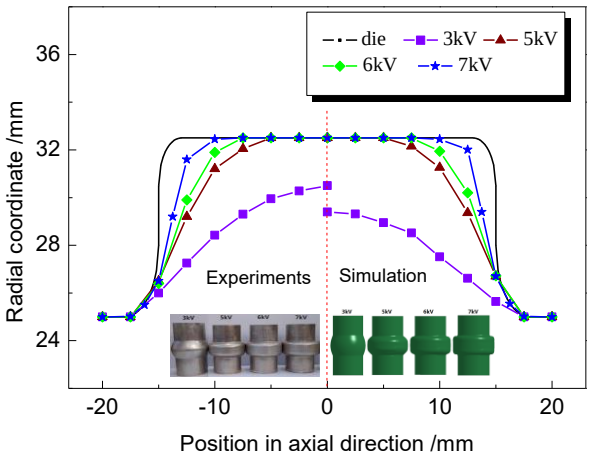

***Figure 10**: Comparison of the experimental and numerical simulation results*

4 Conclusions

In this paper, a numerical model of the EHF process is applied to simulate and analyze the generation and propagation of a shockwave and the plastic deformation behaviour of a tube under the action of the shockwave load during electrohydraulic forming. Further, the resulting stress, displacement and velocity of the tube during the EHF process are discussed quantitatively. Finally, comparing and analyzing the simulation and the experimental results, and obtaining the errors of the two results, it comes out that the

numerical simulations are quite in accordance with the experimental results. Hence, the simulation may provide guidance for further experimental research on the electrohydraulic forming process of tubes.

Acknowledgments

This work was supported by the National Natural Science Foundation of China (Grant No. 51675128, 51475122).The authors would like to take this opportunity to express their sincere appreciation.

References

KangY L, 2008. Lightweight Vehicle, Advanced High Strength Steel and Energy-Saving and Emission Reduction[J]. Iron and Steel, 43 (6): 1-7.

BrunoEJ, 1968. High-velocity Forming of Metals[M]. American Society of Tool and Manufacturing Enerineers, Dearborn.

Gong W S, 1984. Electrohydraulic Forming[J]. New Technology & New Process, 6: 17-18.

Zhang L, Zhou JJ, 1997. Underwater-discharge Forming Technology[C]// Proceedings of the 8th National Symposium on Electrical Processing.

Golovashchenko S F, Gillard A J, Mamutov A V, et al, 2014. Pulsed Electrohydraulic Springback Calibration of Parts Stamped from Advanced High Strength Steel[J]. Journal of Materials Processing Technology.

MelanderA, Delic A, Björkblad A, et al, 2013. Modelling of electro hydraulic free and die forming of sheet steels [J]. International Journal of Material Forming, 6, 223–231.

Hassannejadasl A, Green D E, Golovashchenko S F, et al, 2014.Numerical modelling of electrohydraulic free-forming and die-forming of DP590 steel [J]. Journal of Manufacturing Processes, 16, 391– 404.

Hajializadeh F, Mosavi M M, 2015. Investigation and numerical analysis of impulsive hydroforming of aluminum 6061-T6 tube[J]. Journal of Manufacturing Processes, 20,257– 273.

MamutovA V, Golovashchenko S F, Mamutov V S, et al, 2015.Modeling of electrohydraulic forming of sheet metal parts [J]. Journal of Materials Processing Technology, 219, 84– 100.

Golovashchenko S F, Gillard A J, Mamutov A V, 2013. Formability of dual phase steels in electrohydraulic forming[J]. Journal of Materials Processing Technology,1191-1212.

Golovashchenko S F, Gillard A J, Mamutov AV, et al, 2014.Electrohydraulic trimming of advanced and ultra high strength steels[J]. Journal of Materials Processing Technology, 214,1027– 1043.